Virus Genes (2009) 39:165–175
DOI 10.1007/s11262-009-0382-x

Efficient transduction of cytotoxic and anti-HIV-1 genes by a gene-regulatable lentiviral vector

Yasuhiko Shinoda · Kuniko Hieda · Yoshio Koyanagi · Youichi Suzuki

Received: 18 April 2009 / Accepted: 12 June 2009 / Published online: 25 June 2009

Abstract Lentiviral vectors modified from human immunodeficiency virus type 1 (HIV-1) offer a promising approach for gene therapy, facilitating transduction of genes into non-dividing cells both in vitro and in vivo. When transducing cytotoxic or anti-HIV genes, however, the vector must avoid self-inhibition by the transgene that can lead to a disruption in production of infectious virions. In this study, we constructed two HIV-1-based lentiviral vectors harboring the mifepristone-inducible gene expression unit in either the forward or the reverse orientation with respect to the direction of viral genomic RNA. The ability of these vectors to transduce cytotoxic and anti-HIV genes was evaluated. When human CD14 was used as a transgene, infectious lentiviral vectors were produced by both forward and reverse vector systems. CD14 expression was efficiently induced in cells transduced by both lentiviral vectors following treatment with mifepristone. However, a higher level of basal transgene expression was observed in the forward vector system in the absence of mifepristone. In contrast, high titers of infectious lentiviral vector containing the cytotoxic *vesicular stomatitis virus M* gene were successfully generated using the reverse vector, but not the forward vector. In addition, when a VPS4B-dominant negative mutant against HIV-1 budding was cloned into the reverse vector, significant amounts of lentiviral vector were obtained. Subsequent transduction of cells with the VPS4B mutant resulted in approximately 50% inhibition of HIV-1 production only in the presence of mifepristone. Our study thus demonstrates that incorporation of a mifepristone-regulatable gene expression unit in the reverse orientation makes significant advances toward development of a lentiviral vector that allows transduction of harmful genes.

Keywords Lentiviral vector · Mifepristone-regulatable system · VSV M · VPS4B

Y. Shinoda · K. Hieda · Y. Koyanagi
Laboratory of Viral Pathogenesis, Research Center for AIDS, Institute for Virus Research, Kyoto University, Kyoto 606-8507, Japan

Y. Suzuki (✉)
Laboratory for Host Factors, Center for Emerging Virus Research, Institute for Virus Research, Kyoto University, 53 Shogoin-Kawara-cho, Sakyo-ku, Kyoto 606-8507, Japan
e-mail: ysuzuki@virus.kyoto-u.ac.jp

Present Address:
K. Hieda
Microbiological Research Institute, Otsuka Pharmaceutical Co., Ltd, Kawauchi-cho, Tokushima 771-0192, Japan

Introduction

A variety of gene-transfer vectors based on RNA and DNA viruses have been developed to deliver foreign genes to target cells in vitro and in vivo [1]. Retroviral vectors derived from gammaretroviruses and lentiviruses have the potential advantage of sustained expression of transgenes in transduced cells, because of their ability to stably integrate viral DNA into the host genome. While gammaretroviruses require cell division to establish infections, lentiviruses including human immunodeficiency virus type 1 (HIV-1) are capable of infecting both dividing and non-dividing cells [1]. Lentivirus-based vector systems thus potentiate long-term gene expression in non-dividing cells such as neurons and hematopoietic stem cells [2, 3].

Lentiviral vectors hold great promise for a gene therapy approach to inherited and acquired diseases such as cancer and acquired immunodeficiency syndrome (AIDS).

A potential application of lentiviral vectors would be the transduction of a gene cytotoxic to tumor cells or virus-infected cells resulting in the eradication of these unwanted cells from the body. For the treatment of AIDS, an alternative approach would be to deliver an anti-HIV gene to a population of cells rendering them resistant to HIV infection. However, insertion of toxic or anti-HIV genes into an HIV-based lentiviral vector can create problems for production of the vector itself. Expression of anti-HIV transgenes in vector packaging cells can interfere with production of lentivirus particles, blocking the ability to make lentiviral vector [4]. One strategy to solve this problem is the use of a regulatable system in which the target transgene is kept silent during vector production and expression is subsequently switched on following transduction in the context of a lentiviral vector.

The first generation of regulatable gene expression systems was based on naturally occurring inducible promoters [5]. However, this type of system had limitations due to high levels of "leaky" or basal expression driven by such promoters, modest induction of transgene expression, and pleiotropic activity of the inducer. For these reasons, the last two decades have seen development of chimeric regulatable systems engineered from a number of prokaryotic, eukaryotic, and viral elements designed to enhance specificity and activity of transgene expression [6]. Amongst the reported chimeric regulators is one based on a mutated human progesterone receptor which is unable to bind endogenous hormone but is activated by binding the progesterone antagonist, mifepristone (RU-486) [7, 8]. The chimeric transactivator (regulator) protein of this so-called GeneSwitch system comprises the GAL4 DNA-binding domain from *Saccharomyces cerevisiae* fused to the ligand-binding domain of a mutant progesterone receptor and the activation domain of the p65 subunit of human NF-κB [8]. In the presence of mifepristone, this transactivator binds to GAL4 activation sequences upstream of the inducible transgene, stimulating transcription of the target gene by more than 200-fold in cultured cells [9]. An advantage of the GeneSwitch system is that the majority of its components are modified human proteins having no impact on cell viability. In addition, although mifepristone has anti-progesterone and -glucocorticoid activities, the concentration needed for ligand-inducible transactivation of the target gene (10^{-8} to 10^{-11} M) is much lower than the concentration producing an anti-progesterone effect in humans [10]. Furthermore, use of a mifepristone-inducible (autoinducible) promoter to regulate expression of the chimeric transactivator dramatically reduced basal expression of the transgene in the absence of the inducer, thereby improving the dynamic range of in vivo transgene regulation [9].

Many types of regulatable gene expression systems have been incorporated into lentiviral vectors [11–21]. The most commonly used inducible system is based on the bacterial tetracycline-responsible gene expression system (Tet system) [22]. While representing an important tool for controlling target gene expression, Tet-regulatable systems in the context of lentiviral vectors have shown high basal levels of transgene expression without induction [22]. Such leakiness would be undesirable especially in the production of lentiviral vectors aimed at transducing toxic proteins into target cells.

To generate a viral vector in which transgene expression was tightly controlled, we combined an HIV-1-based lentiviral vector with the GeneSwitch system described above. The mifepristone-inducible lentiviral vector reported here minimized the interference of transgene expression during virus production and permitted efficient transduction of cytotoxic and anti-HIV genes into target cells.

Materials and methods

Cells

GeneSwitch-293 cells (a HEK293-derived human cell line expressing the GeneSwitch protein) were purchased from Invitrogen. GeneSwitch-293 and human 293T cells were maintained in Dulbecco's modified Eagle medium (D-MEM) containing 10% fetal calf serum (FCS), 100 units/ml of penicillin, and 100 μg/ml of streptomycin (D-MEM/10% FCS).

Construction of lentiviral vector plasmids

The mifepristone-inducible promoter sequence, GAL4/TATA, was amplified by polymerase chain reaction (PCR) from the vector pGene/V5-His5C (Invitrogen) and subcloned into LITMUS28 (New England Biolabs) to create pLITMUS28-GAL4/TATA. A GAL4/TATA fragment was then inserted into a Gateway-compatible lentiviral vector plasmid pYK005C [23] producing the plasmid for the forward vector (fragment positioned in the forward orientation).

To generate a plasmid for the reverse vector, a fragment containing the Gateway cloning cassette, internal ribosome entry site (IRES), and humanized *Renilla* green fluorescent protein (hrGFP) sequences together with a fragment containing bovine growth factor hormone poly(A) (BGH pA) sequence were isolated from pYK005C and pSwitch (Invitrogen), respectively. These were subcloned into LITMUS28. Then, the GAL4/TATA sequence derived from pLITMUS28-GAL4/TATA was inserted into the subcloning plasmid. To prepare a vector backbone, the internal human

elongation factor 1 α subunit promoter of a self-inactivating (SIN) lentiviral vector plasmid, CSII-EF-MCS [24], was replaced with a fragment containing GAL4/TATA, Gateway-cassette, IRES, hrGFP, and BGH pA sequences, thus generating the final plasmid.

Preparation of all Gateway plasmids containing the *ccdB* gene was carried out using *Escherichia Coli* (*E. Coli*) strain DB3.1.

Cloning of transgenes

All transgenes were cloned into the lentiviral vector plasmid via the Gateway cloning system [23]. Entry plasmid clones encoding transgenes were constructed as follows. Human CD14 was amplified by PCR using primers containing the *att*B1 tail (5′-GGGGACAAGTTTGTACAAAAAAGCAGGCT-3′) at the 5′-end of the forward primer and the *att*B2 tail (5′-GGGGACCACTTTGTACAAGAAAGCTGGGT-3′) at the 5′-end of the reverse primer [23]. PCR products were subcloned into the entry plasmid, pDONR201 (Invitrogen), using a Gateway BP reaction [23]. Vesicular stomatitis virus matrix protein (VSV M) cDNA fused with a FLAG epitope tag sequence (FLAG-VSV-M) was generated from a VSV M-expressing plasmid, pEGFPN3-M [25]. This involved use of a forward primer containing the *att*B1 tail and subsequent FLAG tag sequence (5′-ATGGATTACAAGGATGACGACGATAAG-3′) and a reverse primer containing the *att*B2 tail. The PCR fragment encoding FLAG-VSV-M was subcloned into entry plasmid, pDONR221 (Invitrogen), by Gateway BP reaction. Fragments encoding the VPS4B K180Q mutant (VPS4B-KQ) or firefly luciferase (Luc) were amplified by PCR from VPS4B K180Q-expressing plasmid [26] and pGL3-Basic (Promega), respectively. These fragments were inserted into *Eco*RI-*Mlu*I sites downstream of three FLAG epitope tags in pCMV-SPORT6-3xFLAG, a Gateway-compatible pCMV-SPORT6 (Invitrogen)-derived entry plasmid. After sequence confirmation, individual transgenes in entry plasmids were transferred to lentiviral vector plasmids by Gateway LR reaction.

Lentiviral vector production

293T cells were seeded to appropriate densities 20 h prior to transfection. Infectious lentiviral vectors pseudotyped with VSV G protein were produced by lentiviral vector plasmid, VSV G- and HIV-1 Rev-expressing plasmid (pCMV-VSV-G-RSV-Rev), and HIV-1 Gag-Pol-expressing plasmid (pCAG-HIVgp) via calcium phosphate-mediated transfection, as described previously [27]. Conditioned medium was harvested 48-h post-transfection and concentrated 40-fold by ultracentrifugation at 4°C at 100,000×*g* for 90 min.

For titration of the lentiviral vectors, GeneSwitch-293 cells were infected with serial dilutions of vector stocks supplemented with 10 nM mifepristone (Invitrogen) 24-h post-infection. Vector titers (transduction units: TU) were determined 48 h after induction by quantitative flow cytometric analysis for hrGFP positive cells.

In the following text, the use of "p" and "v" to prefix nomenclature denotes vector plasmid and infectious lentiviral vector, respectively.

Transduction and induction of transgenes

GeneSwitch-293 cells were seeded in 6-well plates at a density of 1×10^5 cells/well with D-MEM/10% FCS 20 h prior to infection. Cells were then exposed to lentiviral vectors for 24 h at multiplicities of infection (MOI) of 0.1 (for vF-CD14 and vR-CD14) or 5 (for vR-VSV-M). To induce transgene expression, culture medium was replaced with D-MEM/10% FCS containing 10 nM mifepristone and cells were analyzed 48 h (vF-CD14 and vR-CD14 transductions) or 24 h (for vR-VSV-M transduction) later.

Flow cytometric analysis

Transduced cells were incubated with anti-human CD14 mouse monoclonal antibody (61D3, eBioscience) for 20 min at 4°C and then stained with Cy5-conjugated anti-mouse IgG donkey polyclonal antibody (Chemicon International Inc.) for a further 20 min at 4°C. Data were collected using the FACScalibur system (BD Bioscience) and analyzed with WinMDI software.

Western blotting analysis

Cells were lysed in SDS sample buffer (62.5 mM Tris–HCl, pH 6.8, 2% SDS, 5% glycerol, 0.003% bromophenol blue, 0.9% β-mercaptoethanol). Boiled samples were separated by SDS-polyacrylamide gel electrophoresis (SDS-PAGE) and transferred to Immobilion Transfer Membranes (Millipore). Primary antibodies used were (i) anti-FLAG mouse monoclonal IgG (M2, Sigma) to detect FLAG-VSV-M; (ii) biotinylated anti-FLAG mouse monoclonal IgG (BioM2, Sigma) to detect FLAG-VPS4B-KQ and FLAG-Luc; and (iii) anti-α-tubulin mouse monoclonal IgG (DM1A, Sigma) to detect α-tubulin. Biotinylated anti-mouse IgG (BA-2000, Vector Laboratories) was then used for the detection of FLAG-VSV-M. Proteins were detected using horseradish peroxidase (HRP)-conjugated streptavidin (ZYMED Laboratories, for FLAG-tagged proteins) and HRP-conjugated anti-mouse IgG (Cell Signaling, for α-tubulin) using a Western Lightning Chemiluminescence Reagent Plus

(PerkinElmer). Signals were analyzed using a luminescence image analyzer, LAS-3000mini (Fujifilm).

Microscopy analysis

293T cells transfected with pF-VSV-M and pR-VSV-M were examined by light and fluorescent microscopy using an Eclipse TS100 microscope (Nikon) at the point of harvesting lentiviral vector. Images were obtained with a DFC480 digital camera and IM500 image manager software (Leica Microsystems).

To detect FLAG-VSV-M, transduced cells were fixed with 4% paraformaldehyde and incubated with PBS containing 5% normal goat serum and 0.05% Triton X-100 at room temperature for 1 h. This was followed by incubation with anti-FLAG-mouse monoclonal IgG (M2) at 4°C overnight. Samples were then incubated with Alexa Fluor 594-conjugated anti-mouse IgG (Invitrogen) at room temperature for 1 h and nuclei were stained using Hoechst 33342 (Invitrogen). Images were obtained using a CTR 6500 fluorescent microscope and FW4000 software (Leica Microsystems).

Assay for HIV-1 release from VPS4B mutant-transduced cells

GeneSwitch-293 cells were seeded at a density of 1×10^3 cells/well in a 96-well plate 20 h prior to infection and exposed to vR-VPS4B-KQ and vR-Luc at a MOI of 1 for 24 h. Transduced cells were then expanded for 4–5 weeks and reseeded at a density of 4×10^6 cells in a 15-cm diameter dish 20 h prior to induction. A portion of transduced cells was subjected to flow cytometric analysis to monitor hrGFP expression after induction with 10 nM mifepristone. To enrich transduced cells, single hrGFP positive cells were positively selected using the FACSAria cell sorting system (BD Bioscience). Sorted cells were cultured for a further 4–5 weeks and cell clones with the strongest hrGFP signals in respective transductions were used for an assay of HIV-1 release.

For the assay of HIV-1 release, 4 μg of pNL4-3 [28] was transfected to transduced cells with Lipofectamine 2000 (Invitrogen). Four hours post-transfection, culture medium was replaced with D-MEM/10% FCS containing 10 nM mifepristone. Culture supernatant was harvested 24 h later and virus production was monitored by HIV-1 $p24^{CA}$ enzyme-linked immunosorbent assay (ELISA, ZeptoMetrix).

Statistical analysis

Student's t test was used to determine statistical significance. A P value of <0.05 was considered significant.

Results

Generation of mifepristone-inducible lentiviral vectors

To establish a regulatable viral vector system, we cloned a mifepristone-inducible promoter sequence (as an internal promoter) into a self-inactivating (SIN) lentiviral vector plasmid in which the U3 region of the 5′-long terminal repeat (LTR) was replaced with the cytomegalovirus (CMV) promoter and the enhancer/promoter unit was deleted from the U3 region of the 3′-LTR [23, 27]. The inducible promoter was a hybrid consisting of the yeast GAL4 upstream activating sequences linked to the adenovirus major late E1b TATA box (GAL4/TATA) [7]. Gene expression from the GAL4/TATA promoter was controlled by a chimeric regulatory protein termed GeneSwitch. Binding of mifepristone to GeneSwitch induced a conformational change in the regulator to an active state, resulting in transcription of the gene of interest [7]. Besides an inducible promoter, our lentiviral vectors contained a Gateway cloning system reading frame cassette, facilitating cloning of genes of interest by site-specific recombination-based Gateway technology [23]. In addition to a conventional lentiviral vector containing the GAL4/TATA-Gateway component in the forward orientation (forward vector, Fig. 1a), we also constructed a version of the lentiviral vector plasmid in which the inducible gene expression unit was located in the reverse orientation, with the intention of reducing interference from the CMV promoter (reverse vector, Fig. 1a).

To evaluate our gene delivery system, the human *CD14* gene was cloned into both forward and reverse vector plasmids (designated pF-CD14 and pR-CD14, respectively). Infectious lentiviral vectors (vF-CD14 and vR-CD14) were produced following co-transfection of VSV G/Rev-expressing plasmid and Gag-Pol-expressing plasmid into 293T cells. Flow cytometric analysis of transfected cells showed that even in the absence of the GeneSwitch protein and mifepristone, expression of *CD14* and cistronic *hrGFP* genes occurred in pF-CD14-transfected producer cells (40.7 ± 3.1%), while such expression was repressed in pR-CD14-transfected cells (1.4 ± 0.4%) (Fig. 1b). This leaky expression of transgenes from the forward vector plasmid in virus producer cells might be due to transcriptional interference arising from the presence of a heterologous promoter in the same orientation (i.e., the CMV promoter), which was required for Tat-independent transcription of the viral RNA genome [27]. Culture supernatant containing the lentiviral vector was harvested and viral titer determined by quantification of the number of hrGFP-positive cells in viral vector-transduced GeneSwitch-293 cells, expressing the GeneSwitch regulatory protein, in the presence of mifepristone [8]. Lentiviral vectors produced by pF-CD14 showed 34.4-fold higher

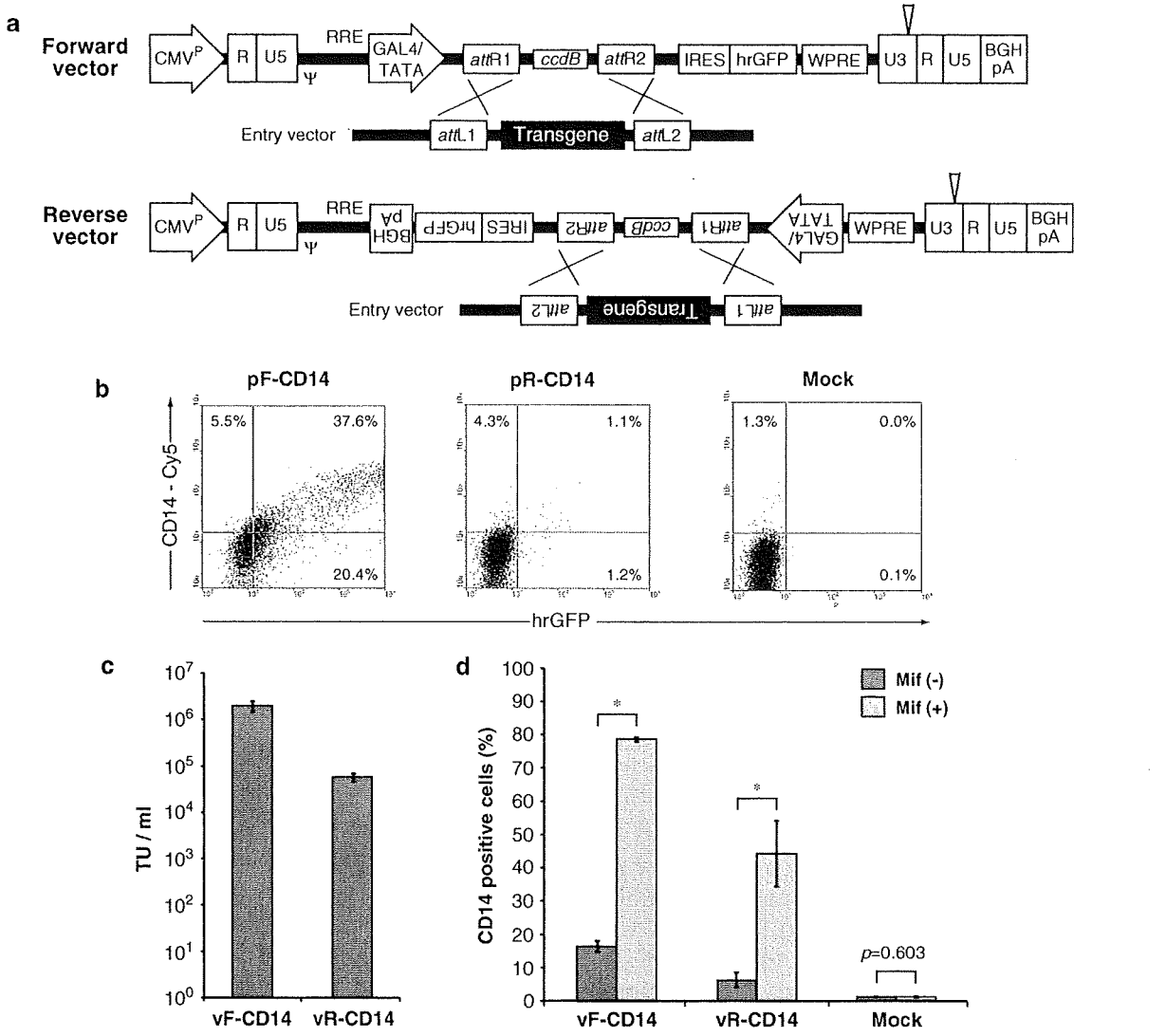

Fig. 1 Transduction of the *CD14* gene by mifepristone-inducible lentiviral vectors. **a** Schematic of forward and reverse vectors. In these SIN lentiviral vector plasmids, the U3 region of the 5′-LTR has been replaced with the CMV promoter (CMV^P) resulting in Tat-independent transcription. A portion of the U3 region containing the enhancer/promoter unit has been deleted from the 3′-LTR (represented as *triangles*). The gene of interest (transgene), flanked by *att*B sites, was subcloned into an entry plasmid and then transferred to the vector plasmid by a Gateway reaction. Note that site-specific recombination between *att*R sites on the vector plasmid and *att*L sites on the entry vector gave rise to new *att*B sites on the final lentiviral vector plasmid. The GAL4/TATA promoter regulated expression of the transgene and IRES-controlled hrGFP gene in the presence of the transactivator protein (GeneSwitch) and mifepristone. Ψ, packaging signal; *RRE* Rev responsive element; *WPRE* woodchuck post-regulatory element, *BGH pA* bovine growth factor hormone poly(A). **b** Expression of CD14 in vector producer cells. 293T cells were co-transfected with a VSV G/Rev-expressing plasmid, a Gag-Pol-expressing plasmid, and a forward or reverse vector plasmid coding *CD14* and *hrGFP* genes (pF-CD14 and pR-CD14, respectively). Expression of CD14 (*y*-axis) and hrGFP (*x*-axis) at the time of vector harvest (48 h after transfection) was analyzed by flow cytometric analysis. Untransfected cells (mock) served as a negative control. The representative results of three independent experiments are shown. **c** Infectious titers of lentiviral vectors. Vector titer (transducing units [TU]/ml) was determined by quantitative flow cytometric analysis for hrGFP positive cells on transduced GeneSwitch-293 cells in the presence of mifepristone. Values represent the mean ± standard deviation (SD) for triplicate determinations. **d** Transduction and induction activities of lentiviral vectors. GeneSwitch-293 cells were infected with vF-CD14 or R-CD14 at a MOI of 0.1 (or uninfected, mock) and cultivated in the presence or absence of 10 nM mifepristone (Mif (+) and Mif (−), respectively). Expression of CD14 protein 48 h after induction was determined by flow cytometric analysis. Values represent the mean ± SD of three independent experiments. The *P* value versus no mifepristone treatment is <0.05 by Student's *t* test (*)

viral titers (vF-CD14, 2.0 ± 0.5 × 10^6 TU/ml) than viral vectors obtained by pR-CD14 (vR-CD14, 5.8 ± 1.1 × 10^4 TU/ml) (Fig. 1c). The transduction and induction efficiencies of lentiviral vectors were then assessed following infection of GeneSwitch-293 cells at a MOI of 0.1. As shown in Fig. 1d, a low level of CD14 expression in

transduced cells was observed in both vF-CD14- and vR-CD14-infected cells in the absence of mifepristone. However, basal gene expression in vF-CD14-infected cells (16.5 ± 1.7%) was higher than that recorded in vR-CD14-infected cells (6.3 ± 2.2%), indicating that transgene expression from the reverse orientation vector was tightly controlled in both transduced cells and virus producer cells (Fig. 1b, d). In the presence of mifepristone, expression of CD14 increased significantly, with the percentage of CD14-positive cells rising to 78.6 ± 0.6% (vF-CD14) and 44.3 ± 9.9% (vR-CD14) (Fig. 1d). The regulation factor (ratio of maximal induced expression to basal expression levels in the absence of the inducer [29]) of vR-CD14 was higher than that of vF-CD14 (7.0-fold vs. 4.7-fold). These results demonstrated that our mifepristone-inducible lentiviral vectors functioned as an efficient gene-delivery system with a tight on–off switch for regulating transgene expression.

Transduction of a cytotoxic gene by the mifepristone-inducible lentiviral vector

In gene therapies for cancer patients, delivery of a cytotoxic gene by lentiviral vector is one strategy for destroying tumor cells. However, expression of a toxic gene in a lentiviral vector genome would hamper vector production resulting in a reduction in titer. Expression of such a cytotoxic gene thus needs to be blocked during the process of vector production. The lentiviral vector described here, containing a mifepristone-inducible gene expression unit in the reverse orientation, shows great promise as a carrier for a cytotoxic transgene with CD14 expression tightly repressed in pR-CD14-transfected producer cells (Fig. 1b). We examined this system further to ascertain if it could produce infectious lentiviral vector containing a cytotoxic gene and transduce that gene into target cells. Forward and reverse vector plasmids containing FLAG tag-fused VSV matrix protein (FLAG-VSV-M) were constructed (pF-VSV-M and pR-VSV-M, Fig. 2a) and transfected into 293T cells to produce VSV G-pseudotyped infectious vector. VSV M was chosen as it inhibits nuclear export of cellular RNA by interacting with nucleoporin. This protein is responsible for most of the cytopathic effects observed in VSV-infected cells [30]. Analysis of the level of FLAG-VSV-M in virus producer cells showed that, even in the absence of inducers, transgene expression was activated in pF-VSV-M-transfected cells, while expression was undetectable in pR-VSV-M-transfected cells (Fig. 2b). As predicted by Western blotting analysis, activated expression of the downstream *hrGFP* cistron, together with the rounded phenotype of infected cells (a hallmark of VSV infection in cell culture [30]), was observed in pF-VSV-M-transfected cells (Fig. 2c). In contrast, pR-VSV-M-transfected cells exhibited neither hrGFP expression nor cytopathic effect, demonstrating the ability of the reverse vector to suppress the cytotoxic gene in virus producer cells (Fig. 2c). Importantly, the ability of pR-VSV-M to suppress VSV M expression was reflected in the production of infectious lentiviral vector from transfected cells. Transfection with pR-VSV-M yielded lentiviral vector (vR-VSV-M) with titers of 1.5 ± 0.5 × 10^4 TU/ml, while no infectious vector could be obtained by transfection with pF-VSV-M (Fig. 2d). The ability of vR-VSV-M to transduce the transgene was then analyzed by infection of GeneSwitch-293 cells. Immunostaining analysis indicated that FLAG-VSV-M expression was induced in response to mifepristone in transduced cells (Fig. 2e) and the regulation factor (i.e., inducibility) was 11.8-fold (FLAG positive cells per Hoechst 33342 positive cells, 4.6 ± 3.2% without mifepristone treatment versus 54.5 ± 20.6% with mifepristone treatment (Fig. 2f). These data demonstrated that our reverse vector system is suitable for the transduction of a harmful gene.

Fig. 2 Effective transduction of VSV M by the reverse vector. ▶ **a** Forward and reverse vectors containing FLAG-tagged VSV M (FLAG-VSV-M) as a transgene (pF-VSV-M and pR-VSV-M, respectively). **b** Expression of FLAG-VSV-M in vector producer cells. 293T cells were co-transfected with a VSV G/Rev-expressing plasmid, a packaging plasmid, and pF-VSV-M or pR-VSV-M to produce lentiviral vectors. Cell extracts were prepared 48 h after transfection and subjected to Western blotting (WB) analysis using anti-FLAG (*upper panel*) and anti-α-tubulin (*lower panel*) antibodies. **c** Leaky expression of VSV M caused the death of producer cells. Fluorescent (*upper panels*) and light (*lower panels*) microscopic analysis of producer cells was undertaken at the time of vector harvest. Scale bar, 40 μm. **d** Titers of lentiviral vectors bearing the *VSV M* gene. TU was determined by hrGFP positive cells in GeneSwitch-293 cells in the presence of mifepristone. The expression of hrGFP in vF-VSV-M-infected cells was below the detection limit (not detected, N.D.). Value of vR-VSV-M represents the mean ± SD of three independent experiments. **e** Inducible expression of FLAG-VSV-M in vR-VSV-M-transduced cells. GeneSwitch-293 cells were infected with vR-VSV-M at a MOI of 5 and fixed with paraformaldehyde 24 h after induction. Expression of FLAG-VSV-M was examined as described in materials and methods. Hoechst 33342 indicates nucleus. Mif (−), without mifepristone treatment; Mif (+), with 10 nM mifepristone treatment; scale bar, 100 μm. **f** Quantification of inducibility. FLAG-VSV-M positive cells observed by immunofluorescence analysis were counted in a randomly selected visual field. Data are expressed as the percentage of $FLAG^+$ cells in Hoechst 33342^+ cells (mean ± SD of four independent transductions). The *P* value versus no mifepristone treatment is <0.05 by Student's *t* test (*)

Inhibition of HIV-1 release by mifepristone-inducible lentiviral vector

To evaluate whether the reverse vector could overcome self-inhibition caused by an anti-HIV transgene in producer cells, a dominant negative mutant of human VPS4B was

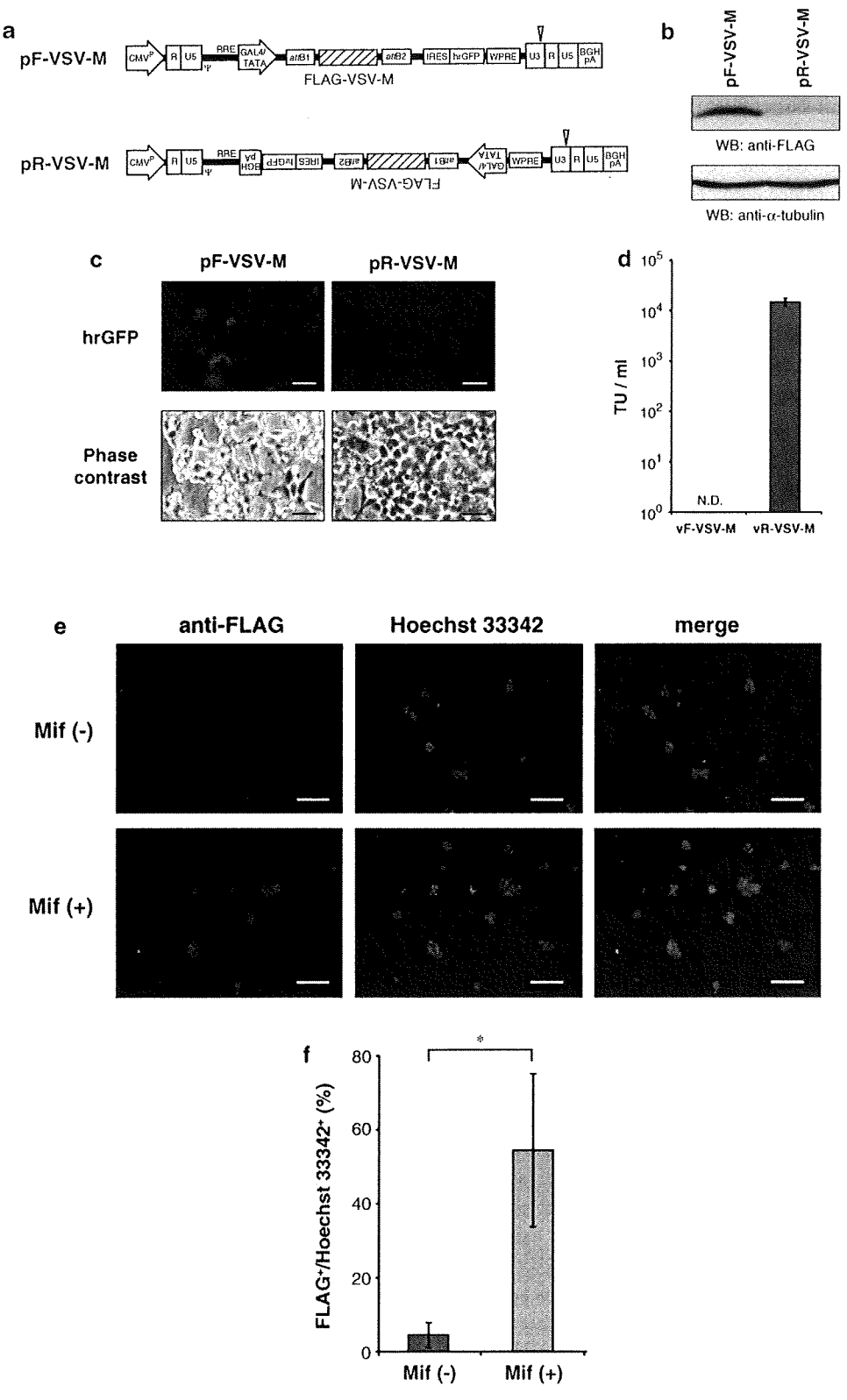

selected as a transgene. VPS4B is one of two known isoforms of AAA-ATPase VPS4 and is thought to catalytically remove endosomal sorting complex required for transport (ESCRT) complex III proteins from the plasma membrane, resulting in budding of HIV-1 from infected cells [26]. The ATPase activity of VPS4B is essential for

HIV-1 budding with dominant negative mutants of VPS4 (such as K180Q, where the residues required for ATP binding have been mutated), previously reported to block HIV-1 release and infectivity [26]. We inserted a FLAG tag-fused VPS4B K180Q mutant (FLAG-VPS4B-KQ) into both the forward and the reverse vector plasmids and constructed vector plasmids encoding FLAG tag-fused luciferase (FLAG-Luc) as control vectors (Fig. 3a). When these vector plasmids were used to produce lentiviral vector, expression of the transgenes (i.e., FLAG-VPS4B-KQ or FLAG-Luc) was observed in producer cells transfected with forward vector plasmids, but not in cells with reverse vector plasmids (Fig. 3b). While transfection with pR-VPS4B-KQ yielded infectious lentiviral vector, vR-VPS4B-KQ, transfection with pF-VPS4B-KQ did not generate infectious vector, indicating that leaky expression of the VPS4 dominant negative mutant from the forward vector plasmid self-inhibited lentiviral vector production (Fig. 3c). Titers of vR-VPS4B-KQ ($8.7 \pm 2.4 \times 10^4$ TU/ml) were comparable to those of lentiviral vector obtained by transfection with pR-Luc (vR-Luc, $5.9 \pm 4.1 \times 10^4$ TU/ml), indicating that titers of lentiviral vectors containing the gene

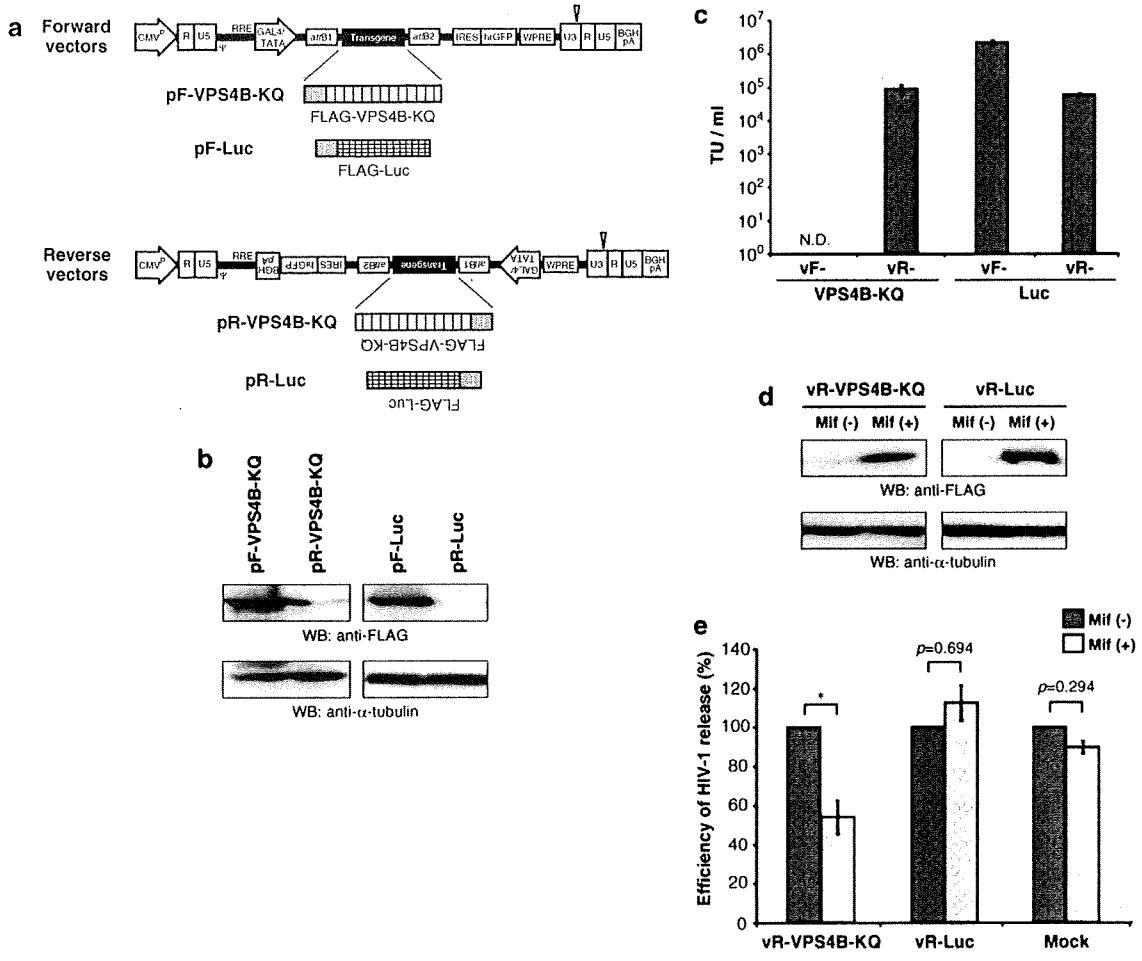

Fig. 3 Inhibition of HIV-1 release by a reverse vector encoding VPS4B dominant negative mutant. **a** Schematic representation of forward and reverse vectors bearing FLAG-tagged VPS4B K180Q (FLAG-VPS4B-KQ) or luciferase (FLAG-Luc). **b** Expression of transgenes in vector producer cells. The lentiviral vectors were produced as described in "Materials and methods". Producer cells were collected at the time of virus harvest and subjected to Western blotting (WB) analysis using anti-FLAG (*upper panels*) and anti-α-tubulin (*lower panels*) antibodies. **c** Titers of lentiviral vectors. N.D. means below the detection limit of flow cytometric analysis for hrGFP expression. **d** Induction of FLAG-VPS4B-KQ and FLAG-Luc expressions by reverse vectors. GeneSwitch-293 cells were infected with vR-VPS4B-KQ or vR-Luc at a MOI of 1 and cultivated in the absence of mifepristone. After sorting of cell clones that were capable of expressing hrGFP, the inducibility of FLAG-VPS4B-KQ and FLAG-luciferase expression was analyzed by western blotting. Mif (−) and Mif (+) indicate before and after induction with mifepristone, respectively. **e** Analysis of HIV-1 production in transduced cells. GeneSwitch-293 cell lines transduced with either vR-VPS4B-KQ or vR-Luc (and untransduced cells, mock) were transiently transfected with pNL4-3. The amount of HIV-1 virions present in the culture supernatant was measured by $p24^{CA}$ ELISA. The efficiency of HIV-1 release in the presence of 10 nM mifepristone is shown as a percentage of the value in the absence of mifepristone (mean ± SD of three independent transfections). The *P* value versus no mifepristone treatment is <0.05 by Student's *t* test (*)

expression unit in a reverse orientation were not affected by the anti-HIV transgene (Fig. 3c).

The ability of our lentiviral vectors to transduce the VPS4B dominant negative mutant for inhibition of HIV-1 release was then tested. GeneSwitch-293 cells were infected with vR-VPS4B-KQ and vR-Luc and sorted for hrGFP positive cells. When transduced cells were cultured with mifepristone, induction of transgene expression was seen (Fig. 3d). The inhibitory effect of transgenes on HIV-1 release from transduced cells was examined by transiently transfecting a plasmid DNA producing infectious HIV-1 virions (pNL4-3). In the presence of mifepristone, levels of HIV-1 production from vR-VPS4B-KQ-transduced cells dropped to 53.9 ± 8.5%, approximately half that seen in the absence of mifepristone treatment. However, no significant inhibitory effects on HIV-1 release were observed in vR-Luc or mock-transduced cells (112.3 ± 9.0% and 89.7 ± 3.1%, respectively). This indicated that induced expression of dominant negative mutant VPS4B proteins in transduced cells accounted for the observed inhibition of HIV-1 release. These results demonstrate the utility of our reverse vector to transduce an anti-HIV gene that functionally suppresses HIV-1 release in target cells.

Discussion

The basic principle of current gene therapy is to deliver genetic material to a population of cells in the body, thereby preventing a disease or improving the clinical status of a patient. Although, a key factor in successfully implementing gene therapy is the development of effective vector systems, a number of issues need to be addressed to apply them in a clinical setting. In terms of viral vector systems, one of the major problems is that insertion of cytotoxic or antiviral transgenes adversely affects viral titers during vector production. In this study, we incorporated a mifepristone-inducible gene expression unit into HIV-1-based lentiviral vectors to solve the problem of vector self-inhibition.

Previous studies have reported the delivery of various anti-HIV genes by HIV-1-based vectors in vitro and in vivo [31–36]. Some of the transgenes used in these studies target HIV-1 RNA sequences either directly or indirectly, aiming to inhibit transcription, nuclear translocation, or translation of viral RNA [32–36]. In these types of approach, the problem of self-inhibition can be solved by modifying the nucleotide sequence of a lentiviral vector such that the function of the vector RNA does not interfere with the anti-HIV transgene in producer cells. However, if the transgene targets a fundamental process of the HIV-1 life cycle, such as virion formation, another strategy to avoid self-inhibition is to express the transgene in a regulated manner such that its expression is blocked in producer cells and induced in target cells. This kind of approach would be of value in the transduction of a harmful gene into target cells. The data presented here demonstrate that a lentiviral vector bearing a regulatable gene expression unit is indeed capable of transducing cytotoxic (VSV M) and anti-HIV (VPS4B K180Q) genes into target cells without significant decrease in vector titer (Figs. 2, 3). In addition, induction of anti-HIV genes in transduced cells resulted in approximately 50% inhibition of HIV-1 release (Fig. 3e).

Expression of VPS4B-KQ mutant by transfection has been reported to inhibit HIV-1 release >100-fold [26]; although, the VPS4B-KQ expression induced by our mifepristone-regulatable system produced about 2-fold reduction in HIV-1 production (Fig. 3e). When we looked at the IRES-controlled hrGFP expression in mifepristone-induced cells that had been transduced by vR-VPS4B-KQ or vR-Luc and sorted, hrGFP expressions were only observed in 10.5% (vR-VPS4B-KQ) or 12.2% (vR-Luc) of the cells (data not shown). We speculate that uninducible population of cells was still permissive to HIV-1 production and thus lead to the observed 50% inhibition in the vR-VPS4B-KQ-transduced cells. During expansion of these transduced cells after cell sorting it is possible that some (e.g., gene shut-off) lost their ability to be induced by mifopristone. Besides, the cell sorting step might lead to this issue of lost inducibility. Therefore improving the way to enrich transduced cells should help to alleviate this problem.

To achieve tight regulation of transgene expression, enabling production of infectious vectors, it was necessary to place the mifepristone-inducible gene expression unit in the reverse orientation in the context of the lentiviral vector. Sirin and Park [12] tested the forward and the reverse orientations of a mifepristone-inducible gene expression unit in HIV-1-based lentiviral vectors and reported basal levels of transgene expression that were higher in lentiviral vectors bearing the expression cassette in the reverse orientation than those containing it in the forward orientation. This was in contrast to the findings presented here, where basal expression of the CD14 transgene in reverse vector-infected cells appeared to be lower than that in forward vector-infected cells (Fig. 1d). Similarly to the Sirin and Park [12] study, we used an HIV-1-based SIN vector in which the woodchuck post-regulatory element (WPRE) was inserted into the 3′-untranslated region of the viral genome (Fig. 1a). WPRE has been reported to increase the stability of RNA transcripts, thereby enhancing transgene expression from retroviral and lentiviral vectors [37]. Interestingly, WPRE functions only when placed in the sense orientation of a transgene and antisense WPRE actually shows an inhibitory effect on transgene expression [37]. In our reverse vector, WPRE

was positioned in the opposite orientation to the inducible gene expression unit (Fig. 1a), while the vector designed by Sirin and Park [12] contained WPRE in same orientation as the expression unit. Orientation-dependent elements such as WPRE can thus enhance basal expression of a transgene in both producer and transduced cells. In addition to WPRE, the SIN vector used in our study contained a hybrid 5′-LTR in which the U3 region was replaced with the CMV promoter [27]. We speculate that, in the context of our forward vector, these *cis*-acting sequences should increase background activity of the mifepristone-regulatable gene expression unit without induction, leading to leaky expression of cytotoxic/anti-HIV genes in producer cells and significant loss of vector titers (Figs. 2d, 3c).

One general drawback of regulatable gene expression systems, including the Tet and mifepristone systems, is that they necessitate delivery of two expression units into a target cell; one to express the transactivator and the other to express the transgene in response to the activator. To exclude differences in experimental conditions due to differing levels of transactivator expression, a cell line stably expressing the GeneSwitch transactivator was used as a target cell in this study. While Sirin and Park [12] also described a two-lentiviral vector system in which GeneSwitch and inducible gene expression units were cloned into separate vectors, this type of binary approach would produce populations of singly transduced cells with either transactivator or transgene, resulting in low inducibility. Single-lentiviral vectors bearing the entire regulatable unit have been developed in Tet systems [11, 38, 39]. This single-vector approach would be an attractive option for the mifepristone-regulatable system, bypassing the need for co-transduction of target cells with high amounts of virus. However, RNA virus-based vectors, such as lentiviral vectors, are limited in their cloning capacity for larger genes. Theoretically, lentiviral vectors can accommodate 7–7.5 kb of foreign DNA [1], yet this packaging capacity will be decreased by the insertion of additional regulatory sequences. Improvements to the mifepristone system that would allow incorporation of both transactivator and inducible units into a single-lentiviral vector would be necessary to design a more versatile vector.

The mifepristone-regulatable gene expression system reported here has a number of potential advantages that suit it to gene therapy applications in humans. First, the majority of the system consists of modified human proteins with no impact on cell viability. Second, the induction response is specific and rapid. Third, mifepristone is orally effective and the dose required for induction is within the range acceptable for clinical use [10]. Importantly, mifepristone has been approved by the Food and Drug Administration (FDA) for use in humans. Although, no gene regulatory system has yet been approved by the FDA for clinical use, lentiviral vectors in conjunction with a mifepristone-regulatable gene expression system are a promising step toward achieving successful gene therapy.

Acknowledgments We thank Hiroyuki Miyoshi (RIKEN BioResource Center) for providing pCMV-VSV-G-RSV-Rev and pCAG-HIVgp, Elisa Izaurralde (European Molecular Biology Laboratory) for EGFP-fused VSV M-expressing plasmid, and Wesley Sundquist (Department of Biochemistry, University of Utah) for dominant-negative mutant VPS4B-expressing plasmid. We are also grateful to Joanne Martin for proofreading of the manuscript and members of the Laboratory of Viral Pathogenesis and the Laboratory for Host Factors for support of experimental techniques and helpful discussions. This work was supported by grants from the Ministry of Health, Labour and Welfare and the Ministry of Education, Culture, Sports, Science and Technology of Japan.

References

1. I.M. Verma, N. Somia, Nature **389**, 239–242 (1997)
2. L. Naldini, U. Blomer, P. Gallay, D. Ory, R. Mulligan, F.H. Gage, I.M. Verma, D. Trono, Science **272**, 263–267 (1996)
3. H. Miyoshi, K.A. Smith, D.E. Mosier, I.M. Verma, B.E. Torbett, Science **283**, 682–686 (1999)
4. J.A. Taylor, L. Vojtech, I. Bahner, D.B. Kohn, D.V. Laer, D.W. Russell, R.E. Richard, Mol. Ther. **16**, 46–51 (2008)
5. M. Fussenegger, Biotechnol. Prog. **17**, 1–51 (2001)
6. S. Agha-Mohammadi, M.T. Lotze, J. Clin. Invest. **105**, 1177–1183 (2000)
7. Y. Wang, B.W. O'Malley Jr., S.Y. Tsai, B.W. O'Malley, Proc. Natl Acad. Sci. USA **91**, 8180–8184 (1994)
8. M.M. Burcin, G. Schiedner, S. Kochanek, S.Y. Tsai, B.W. O'Malley, Proc. Natl Acad. Sci. USA **96**, 355–360 (1999)
9. R.V. Abruzzese, D. Godin, V. Mehta, J.L. Perrard, M. French, W. Nelson, G. Howell, M. Coleman, B.W. O'Malley, J.L. Nordstrom, Mol. Ther. **2**, 276–287 (2000)
10. J.L. Nordstrom, Steroids **68**, 1085–1094 (2003)
11. T. Kafri, H. van Praag, F.H. Gage, I.M. Verma, Mol. Ther. **1**, 516–521 (2000)
12. O. Sirin, F. Park, Gene **323**, 67–77 (2003)
13. B. Mitta, C.C. Weber, M. Rimann, M. Fussenegger, Nucleic Acids Res. **32**, e106 (2004)
14. S.C. Beutelspacher, N. Ardjomand, P.H. Tan, G.S. Patton, D.F. Larkin, A.J. George, M.O. McClure, Exp. Eye Res. **80**, 787–794 (2005)
15. F. Galimi, E. Saez, J. Gall, N. Hoong, G. Cho, R.M. Evans, I.M. Verma, Mol. Ther. **11**, 142–148 (2005)
16. S. Hartenbach, M. Fussenegger, J. Biotechnol. **120**, 83–98 (2005)
17. H.L. Heine, H.S. Leong, F.M. Rossi, B.M. McManus, T.J. Podor, Methods Mol. Med. **112**, 109–154 (2005)
18. B. Mitta, C.C. Weber, M. Fussenegger, J. Gene Med. **7**, 1400–1408 (2005)
19. K. Okamoto, J. Fujisawa, M. Reth, S. Yonehara, Genes Cells **11**, 177–191 (2006)
20. W. Weber, W. Bacchus, F. Gruber, M. Hamberger, M. Fussenegger, J. Biotechnol. **131**, 150–158 (2007)
21. H. Hurttila, J.K. Koponen, E. Kansanen, H.K. Jyrkkanen, A. Kivela, R. Kylatie, S. Yla-Herttuala, A.L. Levonen, Gene Ther. **15**, 1271–1279 (2008)
22. S. Goverdhana, M. Puntel, W. Xiong, J.M. Zirger, C. Barcia, J.F. Curtin, E.B. Soffer, S. Mondkar, G.D. King, J. Hu, S.A. Sciascia, M. Candolfi, D.S. Greengold, P.R. Lowenstein, M.G. Castro, Mol. Ther. **12**, 189–211 (2005)

23. Y. Kawano, T. Yoshida, K. Hieda, J. Aoki, H. Miyoshi, Y. Koyanagi, J. Virol. **78**, 11352–11359 (2004)
24. H. Kuwata, Y. Watanabe, H. Miyoshi, M. Yamamoto, T. Kaisho, K. Takeda, S. Akira, Blood **102**, 4123–4129 (2003)
25. H. Ebina, J. Aoki, S. Hatta, T. Yoshida, Y. Koyanagi, Microbes Infect. **6**, 715–724 (2004)
26. U.K. von Schwedler, M. Stuchell, B. Muller, D.M. Ward, H.Y. Chung, E. Morita, H.E. Wang, T. Davis, G.P. He, D.M. Cimbora, A. Scott, H.G. Krausslich, J. Kaplan, S.G. Morham, W.I. Sundquist, Cell **114**, 701–713 (2003)
27. H. Miyoshi, U. Blomer, M. Takahashi, F.H. Gage, I.M. Verma, J. Virol. **72**, 8150–8157 (1998)
28. A. Adachi, H.E. Gendelman, S. Koenig, T. Folks, R. Willey, A. Rabson, M.A. Martin, J. Virol. **59**, 284–291 (1986)
29. Z.L. Xu, H. Mizuguchi, T. Mayumi, T. Hayakawa, Gene **309**, 145–151 (2003)
30. H.R. Jayakar, M.A. Whitt, J. Virol. **76**, 8011–8018 (2002)
31. M.R. Mautino, R.A. Morgan, Aids Patient Care STDS **16**, 11–26 (2002)
32. M. Mukhtar, H. Duke, M. BouHamdan, R.J. Pomerantz, Hum. Gene Ther. **11**, 347–359 (2000)
33. M.R. Mautino, R.A. Morgan, Gene Ther. **9**, 421–431 (2002)
34. A. Banerjea, M.J. Li, G. Bauer, L. Remling, N.S. Lee, J. Rossi, R. Akkina, Mol. Ther. **8**, 62–71 (2003)
35. M.J. Li, G. Bauer, A. Michienzi, J.K. Yee, N.S. Lee, J. Kim, S. Li, D. Castanotto, J. Zaia, J.J. Rossi, Mol. Ther. **8**, 196–206 (2003)
36. H. Nishitsuji, T. Ikeda, H. Miyoshi, T. Ohashi, M. Kannagi, T. Masuda, Microbes Infect. **6**, 76–85 (2004)
37. R. Zufferey, J.E. Donello, D. Trono, T.J. Hope, J. Virol. **73**, 2886–2892 (1999)
38. E. Vigna, S. Cavalieri, L. Ailles, M. Geuna, R. Loew, H. Bujard, L. Naldini, Mol. Ther. **5**, 252–261 (2002)
39. R. Vogel, L. Amar, A.D. Thi, P. Saillour, J. Mallet, Hum. Gene Ther. **15**, 157–165 (2004)

Microbiology and Immunology

Microbiol Immunol 2009; **53**: 629–635
doi:10.1111/j.1348-0421.2009.00167.x

ORIGINAL ARTICLE

N-linked glycan-dependent interaction of CD63 with CXCR4 at the Golgi apparatus induces downregulation of CXCR4

Takeshi Yoshida, Hirotaka Ebina and Yoshio Koyanagi

Laboratory of Viral Pathogenesis, Institute for Virus Research, Kyoto University, Sakyo-ku, Kyoto, 606-8507, Japan

ABSTRACT

Efficient downregulation of CXCR4 cell surface expression by introduction of the CD63 gene has previously been reported by us. In the present study, it was found that CD63 and its mutant efficiently interact with CXCR4 in live cells and that CD63-induced downregulation and interaction are significantly abrogated by the *N*-linked glycosylation inhibitor, TM. Furthermore, the downregulation and interaction were clearly attenuated by alternation of all three *N*-linked glycosylation sites in CD63. Either CD63 or CD63ΔN formed a complex with CXCR4 at the Golgi apparatus and the late endosomes, while CD63 GD mutants lost the ability to form a complex with CXCR4 exclusively at the Golgi apparatus. These findings suggest that CD63 interacts with CXCR4 through the *N*-linked glycans-portion of the CD63 protein and that the complex induces direction of CXCR4 trafficking to the endosomes/lysosomes, rather than to the plasma membrane. At the Golgi apparatus, there may be lysosome protein (CD63)-associated machinery that influences trafficking of other membrane proteins.

Key words CXCR4, membrane trafficking, *N*-linked glycosylation, tetraspanin.

At the Golgi apparatus, the cellular sorting machineries govern directing of secretory proteins to either the plasma membrane or to the endosomal system (1). The secretory pathway links organelles together to provide a framework by which proteins undergo a series of posttranslational modifications including folding and glycosylation. *N*-linked glycosylation of proteins is known to be related to chaperone-mediated folding of the polypeptide, thus contributing to quality control in the ER (2). However, it remains unknown whether *N*-linked glycans take part in physiological events within other intracellular compartments.

We previously found that tetraspanin CD63 has an opposing effect on the expression of the chemokine receptor CXCR4(3). CD63ΔN induces severe downregulation of CXCR4 surface expression, and this effect appears to be caused by selective direction of CXCR4 from the Golgi apparatus to the endosomes/lysosomes, rather than to the plasma membrane (3). This suggests that CD63ΔN, probably CD63 itself, might have a role in the control of CXCR4 trafficking to different final destinations.

We show herein that the *N*-linked glycans-portion of CD63 functions as a determinant of alteration of CXCR4 trafficking.

MATERIALS AND METHODS

Expression plasmids

pCXCR4-mKGC (4), phmKGN-MC, (Medical & Biological Laboratories, Nagoya, Japan), pcDNA3.1 and pCMV-SPORT6 (Invitrogen, Carlsbad, CA, USA) were used.

Correspondence
Yoshio Koyanagi, Laboratory of Viral Pathogenesis, Institute for Virus Research, Kyoto University, 53 Shogoin-kawara-cho, Sakyo-ku, Kyoto, 606-8507, Japan.
Tel: 81 75 751 4811; fax: 81 75 751 4812; email: ykoyanag@virus.kyoto-u.ac.jp

Received 21 April 2009; revised 7 July 2009; accepted 20 July 2009.

List of Abbreviations: BiFC, bimolecular fluorescence complementation; CD63ΔN, an N-terminal deletion mutant of CD63; CD63FL, CD63 full length; ceramide, NBD C_5-ceramide; DIC, differential interference contrast; ER, endoplasmic reticulum; FL, full length; GD, *N*-linked glycans-deficient form; GI, glycans-intact form; KG, Kusabira green; KGC-CXCR4, C-terminal KG peptide-tagged CXCR4; KGN-CD63ΔN, N-terminal KG peptide-tagged CD63ΔN; MFI, mean fluorescence intensity; TGN, trans-Golgi network; TM, tunicamycin.

Plasmid DNA expressing GD mutants substituted from Asn to Glu at three *N*-linked glycosylation sites (amino acid position at 130, 150 and 172) of CD63ΔN and CD63FL were generated by overlap extension PCR. An orf fragment of *CD63FL, CD63ΔN* or these GD mutants was inserted into pCMV-SPORT6, downstream sites of N-terminal KGN peptide-tag in phmKGN-MC or FLAG-tag in p3XFLAG-CMV-10 (Sigma, St Louis, MO, USA). An HA-tag was inserted into an upstream site of the CD63 orf fragment in pCMV-SPORT6 by PCR. pCXCR4 is made from SRαLEGFP (5) by replacement of *EGFP* with *CXCR4*. The nucleotide sequences of all plasmids were confirmed using ABI 3100 auto-sequencer.

Cell culture and transfection

293T, MAGIC-5 and MT-4 cells were used as previously described (3). A transIT LT-1 transfection reagent (Mirus Bio, Madison, WI, USA) and the calcium phosphate method were used for DNA transfection into MAGIC-5 and 293T cells, respectively. To measure the extent of suppression of CXCR4 surface expression, 293T cells were co-transfected with either 0.5 μg of GI or 1.5 μg of GD of CD63ΔN plasmid DNA, or either 0.05 μg of GI or 0.15 μg of GD of CD63FL plasmid DNA together with 2 μg of pCXCR4.

Lentiviral vector transduction and HIV-1 infection

A bicistronic $H2K^k$-expressing lentiviral vector and HIV-1 envelope-pseudotyped luciferase-expressing $HIV\text{-}1_{NL-4}$ (NL-luc) were prepared and used as described previously (3,6,7).

Flow cytometry

Staining of CXCR4 was performed as previously described (3). For BiFC assay (8), cells were transfected with 0.5 μg of KGN-tagged GI or 1.5 μg of GD of either CD63FL or CD63ΔN plasmid DNA together with 0.5 μg of pCXCR4-mKGC. Culture media was replaced by media with or without 0.5 μM of TM (Sigma-Aldrich, St. Louis, MO, USA) 12 hr post transfection.

Immunoblotting

CXCR4 and β-actin were detected as previously described (3). Anti-CD63 mAb (Santa Cruz Biotechnology) and anti-KGN mAb (Medical and Biological Laboratories) were also used.

Microscopic analyses

FLAG- and HA-protein, p230, and LAMP-1 were detected as previously described (3). Anti-HA mAb (3F10, Roche, Indianapolis, IN, USA) was used. For live cell imaging, transfected cells were stained with ceramide, Hoechst33342 (Molecular Probes, Eugene, OR, USA) or LysoTracker Blue DND-22 (Molecular Probes). Cells were analyzed using a DMIRE2-TCS SP2 AOBS confocal microscope system (Leica, Heidelberg, Germany) and images were processed using Photoshop CS2 (Adobe).

Statistical analysis

The Mann–Whitney's *U* test and Student's *t*-test were used to determine statistical significance.

RESULTS

Requirement of N-linked glycans of CD63 for downregulation of CXCR4

We initially confirmed clear downregulation of CXCR4 surface expression in CD63ΔN- or CD63FL-transduced MT-4 cells compared to that in empty vector-transduced cells (Fig. 1a, columns of 1 in top) as described previously (3). Next, we examined the effect of an *N*-linked glycosylation inhibitor, TM, on surface expression of CXCR4. Following 12 hr TM treatment, CXCR4 surface expression increased in CD63ΔN- or CD63FL-transduced cells but not in empty vector-transduced cells (Fig. 1a, top columns). Glycosylation of endogenous CD63, ectopically expressed CD63ΔN and CD63FL in the cells were clearly inhibited by TM treatment (Fig. 1a, upper panels). On the other hand, we found similar CXCR4 bands irrespective of TM treatment (Fig. 1a, middle panels). Because the kinetics of newly synthesized CD63 is faster than that of CXCR4 (9,10), following TM treatment glycosylated CD63 seemed to disappear more quickly than glycosylated CXCR4. In addition, we also observed more significant abrogation of CXCR4 downregulation following TM treatment in CD63ΔN-transduced MAGIC-5 cells (Fig. 1b). Since the surface expression of CXCR4 GD mutants is, however, known to be comparable to that of the wild type (11), it is possible that *N*-linked glycosylation in ectopically expressed CD63ΔN and CD63FL is indispensable for CXCR4 downregulation.

To assess this possibility, we generated plasmid DNA expressing GD mutants of CD63ΔN and CD63FL whose three potential *N*-liked glycosylation Asn sites (amino acid position at 130, 150 and 172) were respectively or together substituted with Gln. Western blotting of cells transfected with these GD mutant DNA showed smaller bands compared to those with GI DNA, indicating that all three sites are glycosylated (data not shown). When cells were co-transfected with pCXCR4 and the individual plasmid DNA of these GD mutants, we observed clearly less

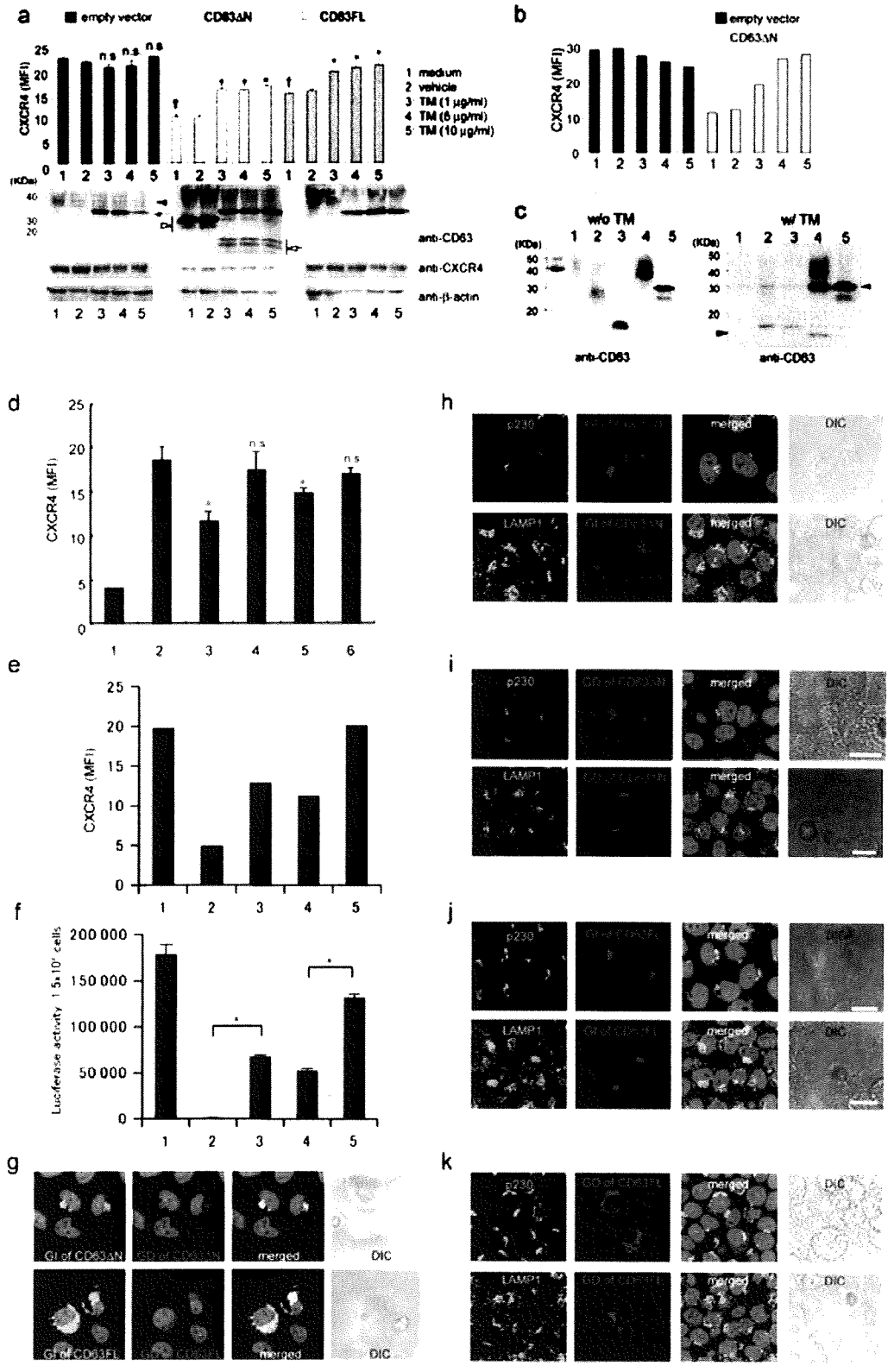

Fig. 1. The importance of the *N*-linked glycans of CD63 for downregulation of CXCR4. (a) Flow cytometric analysis of CXCR4 (MFI in top columns) and Western blotting (lower three panels). Lentiviral vector-transduced MT-4 cells were treated with TM as indicated. Data are represented as mean ±SED, $n = 3$. (Black arrow head) glycosylated CD63FL; (black arrow) unglycosylated CD63FL; (white arrow head) glycosylated CD63ΔN;

downregulation of CXCR4 only in the GD mutants that were substituted at all three *N*-liked glycosylation sites of CD63ΔN and CD63FL though the extent of mutant expression was slightly less as shown by Western blotting (data not shown). To normalize the expression, we transfected cells with more plasmid DNA of GD than that of GI. When the ratio of the DNA of GD to GI was 3 to 1 for CD63FL and CD63ΔN, we obtained an equivalent level of protein expression (Fig. 1c, lanes 2 vs. 3 and 4 vs. 5). Under this condition, we found efficient capability in downregulation for transiently expressed CXCR4 in plasmid DNA expressing GI of CD63ΔN or CD63FL (Fig. 1d, columns 3 and 5), but not in plasmid DNA expressing GD of CD63ΔN or CD63FL (Fig. 1d, columns 4 and 6). The downregulation ability of CD63 GD-expressing lentiviral vectors for endogenous CXCR4 was also clearly attenuated compared to that of CD63 GI-expressing lentiviral vectors (Fig. 1e, lane 2 vs. 3 and 4 vs. 5) under its equivalent transduction efficiency of the lentiviral vectors as shown by staining with anti-$H2K^K$ antibody (data not shown). However, the extent of CXCR4 surface expression on CD63ΔN GD-transduced MT-4 cells was still less than that on empty vector-transduced MT-4 cells.

Correlating to the CXCR4 surface expression on these transduced cells, the HIV-1 susceptibility of GD-transduced MT-4 cells, (examined by CXCR4-using HIV-1 envelope-pseudotyped NL-luc), was clearly greater than that of GI-transduced MT-4 cells (Fig. 1f). On the other hand, distribution of GD mutants in cells was almost identical to that of GI proteins, as shown by dual staining of GI and GD in cells co-transfected with plasmid DNA expressing GD and GI of CD63ΔN and CD63FL (Fig. 1g). In addition, experiments involving staining of GI or GD of CD63ΔN and CD63FL together with antibody against p230 (the TGN marker) or LAMP-1 (the late endosome marker) confirmed that intracellular localization of the GD mutants was unchanged (Fig. 1h–k). Collectively, these data indicate that the *N*-linked glycans-portion of CD63ΔN and CD63FL, not its distribution, may be required for limiting CXCR4 surface expression.

N-linked glycans-dependent interaction of CD63 with CXCR4

We previously detected interaction of CD63ΔN or CD63FL with CXCR4 by immunoprecipitation-Western blotting (3). To confirm the interactions in live cells, we next used a BiFC assay to enable us to visualize the intracellular distribution of specific interactive complexes (8). MAGIC-5 cells were co-transfected with plasmid DNA expressing KGC-CXCR4 and either KGN-CD63ΔN or KGN-CD63FL. We detected CXCR4-CD63ΔN complexes exclusively in the perinuclear regions (Fig. 2a, upper panel), and they appeared to be predominantly distributed at the ceramide$^+$ region (the Golgi apparatus) and LysoTracker$^+$ region (the late endosomes/lysosomes) (Fig. 2a), suggesting that CD63ΔN interacts with CXCR4 mainly at the Golgi apparatus and the late endosomes/lysosomes. In contrast, CXCR4-CD63FL complexes were detected at the plasma membrane as well as in the perinuclear regions (Fig. 2b, upper panel). The perinuclear CXCR4-CD63FL complexes were positively stained with ceramide and Lyso Tracker (Fig. 2b). Thus, the CXCR4-CD63ΔN complex seems to lose the ability to be trafficked to the plasma membrane. When cells were co-transfected with plasmid DNA expressing KGC-CXCR4 and GD of KGN-CD63ΔN, we found significant decrease in signal, which was very

Fig. 1. (white arrow) unglycosylated CD63ΔN; (n.s.) $P > 0.01$ compared to same cells treated with vehicle; (*) $P < 0.01$ compared to same cells treated with vehicle; (†) $P < 0.01$ compared to untreated empty vector-transduced cells. (**b**) Flow cytometric analysis of CXCR4. Lentiviral vector-transduced MAGIC-5 cells were treated as indicated in (a). (**c**) Western blotting of GI and GD of CD63ΔN or CD63FL. 293T cells were transfected with empty vector (lane 1), plasmid DNA expressing GI of CD63ΔN (lane 2), GD of CD63ΔN (lane 3), GI of CD63FL (lane 4), GD of CD63FL (lane 5) and probed with the indicated mAb. (Black arrow head) unglycosylated form of CD63ΔN; (white arrow head) unglycosylated form of CD63FL. (**d**) Flow cytometric analysis of exogenous CXCR4. 293T cells were co-transfected without pCXCR4 and empty vector (column 1), with pCXCR4 and empty vector (column 2), plasmid DNA expressing GI of CD63ΔN (column 3), GD of CD63ΔN (column 4), GI of CD63FL (column 5), GD of CD63FL (column 6) and analyzed 24 hr post transfection. Data are represented as mean ±SED, $n = 6$. (n.s.), $P > 0.01$ as compared to column 2; (*), $P < 0.01$ as compared to column 2. (**e**) Flow cytometric analysis of endogenous CXCR4. (**f**) HIV-1 susceptibility. MT-4 cells were transduced by lentiviral vector of empty vector (column 1), GI of CD63ΔN (column 2), GD of CD63ΔN (column 3), GI of CD63FL (column 4), GD of CD63FL (column 5). (**e, f**) CXCR4 surface expression on these cells and HIV-1 susceptibility was analyzed as described before (3,7). $n = 3$. (*) $P < 0.01$ as compared to column 2 or 4. (**g–k**) Confocal microscopic analysis of GI and GD of CD63ΔN or CD63FL. (**g**) MAGIC-5 cells were co-transfected with either GI of FLAG-CD63ΔN and GD of HA-CD63ΔN plasmid DNA (upper panels) or GI of FLAG-CD63FL and GD of HA-CD63FL plasmid DNA (lower panels) and co-stained with anti-HA and anti-FLAG mAbs. (Red) FLAG-protein; (green) HA-protein; (blue) nuclei. DIC images are also shown. Scale bar, 10 μm. Cells were transfected (**h**) with GI of FLAG-CD63ΔN, (**i**) with GD of FLAG-CD63ΔN, (**j**) with GI of FLAG-CD63FL, or (**k**) with GD of FLAG-CD63FL. These cells were co-stained with antibodies against FLAG (red) and p230 or LAMP-1. (**h-k**). Scale bars, 20 μm.

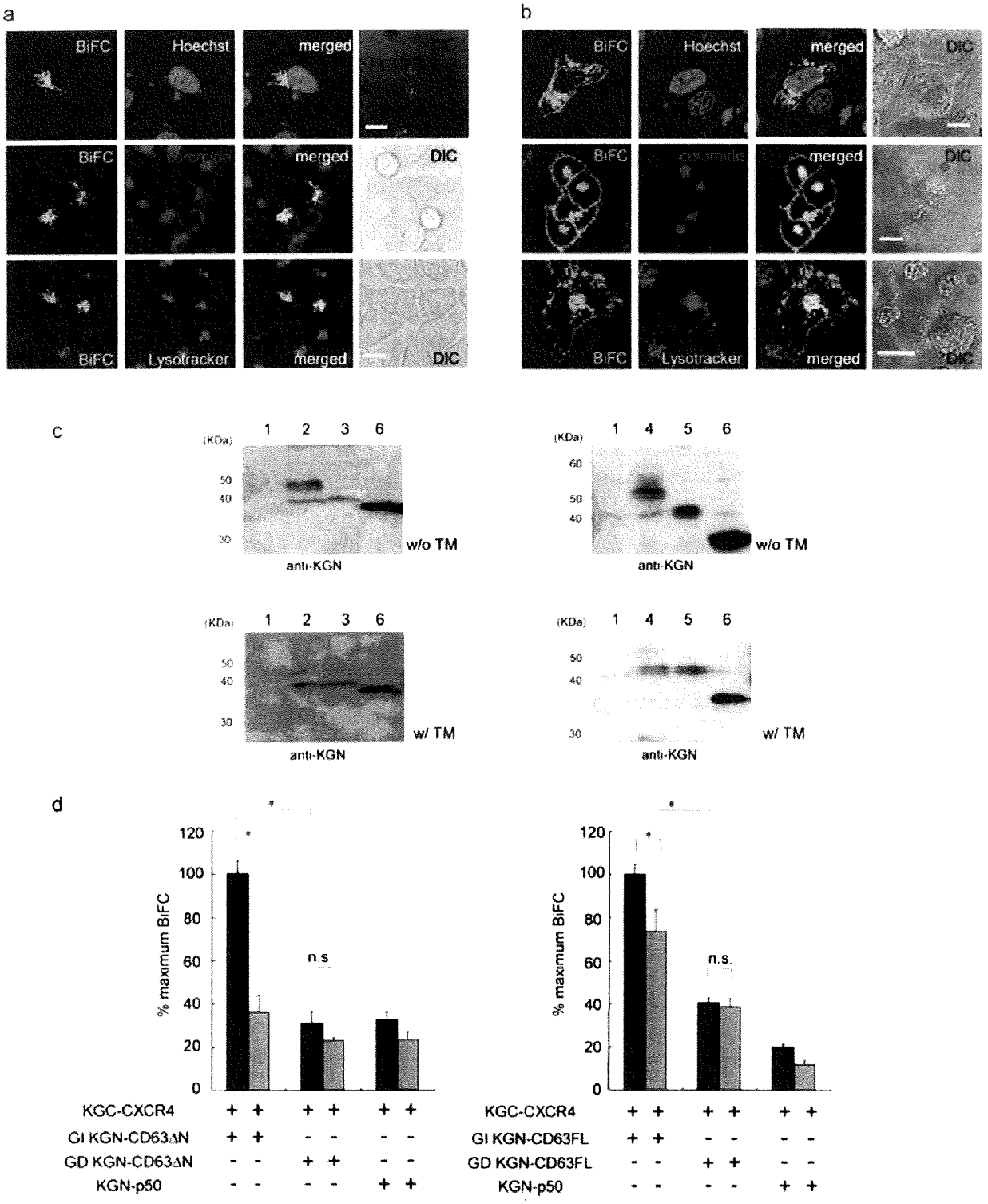

Fig. 2. *N*-linked glycans-dependent interaction of CD63 with CXCR4. (**a**,**b**) BiFC analysis of interaction of CXCR4 with (a) CD63ΔN or (b) CD63FL as shown by confocal microscopy. Scale bars, 10 μm. DIC images are also shown. (**c**) Western blotting of GI and GD of KGN-CD63ΔN or KGN-CD63FL. 293T cells were transfected with pcDNA3.1 (lane 1), plasmid DNA expressing GI of KGN-CD63ΔN (lane 2), GD of KGN-CD63ΔN (lane 3), GI of KGN-CD63FL (lane 4), GD of KGN-CD63FL (lane 5), KGN-p50 (lane 6) and probed with the indicated mAb. (**d**) BiFC analysis of CXCR4 and CD63ΔN or CD63FL measured by flow cytometry. 293T cells were co-transfected with plasmid DNA expressing KGC-CXCR4 and KGN-tagged protein as indicated and cultured in the absence (filled columns) or presence (grey columns) of TM. Y axis

weak and predominantly located at the Lyso Tracker$^+$ region and not the ceramide$^+$ region (data not shown). A similar decrease in signal at the ceramide$^+$ region was also found in the case of the CXCR4-GD of CD63FL complex (data not shown).

To quantify the extent of the interaction, we measured the correlative increase in intensity of the fluorescence signal detected in transfected 293T cells by flow cytometry as increase in plasmid DNA expressing KGN-tagged p50 (an NF-κB subunit) and KGC-tagged p65 (a known interaction protein of p50) but not other unrelated molecules (data not shown), indicating that the intensity of the signal using a single pair of expression plasmids reflects the extent of molecular interaction. Comparison of the BiFC signal of CXCR4-CD63FL (GI and GD) with CXCR4-CD63ΔN (GI and GD) was not evaluated due to the difference in strength of the fluorophore constituent. CXCR4-CD63FL (GI and GD) interaction leads to a more stable fluorophore which emits a stronger signal than the one obtained from the CXCR4-CD63ΔN (GI and GD) interaction, making direct comparisons between associations of CD63FL and CD63ΔN inequitable. Therefore, differences between GI and GD of CXCR4-CD63FL only, or with CXCR4-CD63ΔN only, were assessed.

Under normalized conditions on the expression of GI and GD of KGN- CD63ΔN or KGN-CD63FL (Fig. 2c), we found significant fluorescence between CXCR4 and GI of either CD63ΔN or CD63FL (Fig. 2d), whereas less of a fluorescence signal between CXCR4 and GD of either CD63ΔN or CD63FL was observed (Fig. 2d). We also found significant attenuation in the interaction of CXCR4 with GI of either CD63ΔN or CD63FL by TM treatment, but no change in the signal in interactions between CXCR4 with GD of either CD63ΔN or CD63FL, respectively (Fig. 2d, grey columns), indicating that the *N*-linked glycans-portion of CD63ΔN and CD63FL participates in its efficient interaction with CXCR4. Interestingly, although TM treatment of GI of CD63FL and CD63ΔN attenuated the BiFC signal, interaction with CXCR4 was still observed (Fig. 2d). Moderate interaction was also observed in GD mutants regardless of TM treatment. Taken together, these results indicate that even with abrogation of glycosylation, weak interaction between CXCR4 and CD63FL or CD63ΔN may still occur, however not enough to downregulate the receptor.

DISCUSSION

In the present study, we show that the *N*-linked glycans of CD63 protein mediate its interaction with CXCR4 and that this complex formation can convert the destination of CXCR4 to the late endosomes/lysosomes.

To understand the characteristics of the *N*-linked glycans of CD63, we carried out a series of experiments using both CD63FL and CD63ΔN because CD63FL is a native form of the protein and the effect of CD63ΔN on CXCR4 surface expression is more significant than that of CD63FL ((3) and Fig. 1a). First, we showed that the *N*-linked glycans-portion of CD63FL and CD63ΔN is required to induce efficient downregulation of CXCR4 surface expression (Fig. 1d and e) and to interact with CXCR4 (Fig. 2d). It is well known that glycosylation of membrane protein is a crucial step for its correct folding. However, we clearly detected significant expression of GD of CD63ΔN and CD63FL (Fig. 1c, i, and k). Interestingly, other tetraspanins such as CD9 and CD81, which have no potential glycosylation site, had little suppressive activity for CXCR4 surface expression (3), suggesting that *N*-linked glycans-dependent tetraspanin binding to CXCR4 has a role in regulation of CXCR4 trafficking.

CD63 is well known as a marker of the late endosome/lysosome. Furthermore, we showed that CD63ΔN or CD63FL, including GD mutants, localizes in the TGN (Fig. 1h–k). Correspondingly, CD63 has recently been reported to also localize in the TGN and post-TGN-derived vacuoles (12). Another group has also shown that, in contrast to other secretory proteins, there is a distinct processing period for CD63 maturation in the Golgi apparatus (13). Because we detected significant localization of CD63-CXCR4 complexes at the Golgi apparatus (Fig. 2b), it is possible that Golgi-localized CD63 may have an undiscovered role, such as organizing the destination of other proteins.

We originally found CD63ΔN-CXCR4 or CD63FL-CXCR4 complexes by biochemical methods (3) and confirmed their presence in live cells using the BiFC technique (Fig. 2a and b). According to results of transient co-transfection experiments using the same amount of plasmid DNA, the level of CXCR4-CD63ΔN BiFC signal seemed to be weaker than that of CXCR4-CD63FL. Due to differences in the orientation of the BiFC fragments, compared to CD63FL and CXCR4, the MFI produced by

Fig. 2. indicates % of maximum BiFC, which is defined by dividing the MFI values of BiFC interactions by the maximum obtainable MFI from the interaction between CXCR4 and GI of CD63ΔN (left panel) or CD63FL (right panel) in the absence of TM. Data are represented as mean ±SED, $n = 4$. (n.s.), $P > 0.01$; (*), $P < 0.01$.

the interaction of CD63ΔN with CXCR4 may not be able to reach the same maximum intensity. Perhaps the interaction between CD63FL and CXCR4 allows for a more stable fluorophore constitution, whereas the interaction between CD63ΔN and CXCR4 doesn't as a result of different binding affinities or conformational changes of the FL versus the deletion mutant interaction with CXCR4. Therefore, we plotted the two interaction pairs separately and showed that, when compared to the GI CD63 variants not treated with TM, interaction with CXCR4 was significantly reduced when GD CD63 variants were transfected instead of GI CD63FL or CD63ΔN (Fig. 2d).

Detection of the CD63FL-CXCR4 complex at the plasma membrane (Fig. 2b) suggests the possibility that CXCR4 is transported together with CD63 protein. Trafficking efficiency of the CD63FL-CXCR4 complex to the plasma membrane seems to be more significant than that of the CD63ΔN-CXCR4 one. This preferential trafficking of CD63FL may explain the weaker activity of CD63FL for CXCR4 downregulation.

ACKNOWLEDGMENTS

We thank the many colleagues who have contributed ideas and help to this project, in particular Dr. Jun Komano, Mr. Peter Gee for discussion and Ms. Misawa for assistance. This work was supported by grants from the Ministry of Health, Labor, and Welfare and the Ministry of Education, Culture, Sports, Science and Technology of JAPAN. T. Y. is a research fellow of the Japan Society for the Promotion of Science.

REFERENCES

1. van Vliet C., Thomas E.C., Merino-Trigo A., Teasdale R.D., Gleeson P.A. (2003) Intracellular sorting and transport of proteins. *Prog Biophys Mol Biol* **83:** 1–45.
2. Zhao Y.Y., Takahashi M., Gu J.G., Miyoshi E., Matsumoto A., Kitazume S., Taniguchi N. (2008) Functional roles of N-glycans in cell signaling and cell adhesion in cancer. *Cancer Sci* **99:** 1304–10.
3. Yoshida T., Kawano Y., Sato K., Ando Y., Aoki J., Miura Y, Komano J., Tanaka Y., Koyanagi Y. (2008) A CD63 mutant inhibits T-cell tropic human immunodeficiency virus type 1 entry by disrupting CXCR4 trafficking to the plasma membrane. *Traffic* **9:** 540–58.
4. Hamatake M., Aoki T., Futahashi Y., Urano E., Yamamoto N., Komano J. (2009) Ligand-independent higher-order multimerization of CXCR4, a G-protein-coupled chemokine receptor involved in targeted metastasis. *Cancer Sci* **100:** 95–102.
5. An D.S., Koyanagi Y., Zhao J.Q., Akkina R., Bristol G., Yamamoto N., Zack J.A., Chen I.S.Y. (1997) High-efficiency transduction of human lymphoid progenitor cells and expression in differentiated T cells. *J Virol* **71:** 1397–404.
6. Kawano Y., Yoshida T., Hieda K., Aoki J., Miyoshi H., Koyanagi Y. (2004) A lentiviral cDNA library employing lambda recombination used to clone an inhibitor of human immunodeficiency virus type 1-induced cell death. *J Virol* **78:** 11352–59.
7. Sato K., Aoki J., Misawa N., Daikoku E., Sano K., Tanaka Y., Koyanagi Y. (2008) Modulation of human immunodeficiency virus type 1 infectivity through incorporation of tetraspanin proteins. *J Virol* **82:** 1021–33.
8. Ghosh I., Hamilton D., Regan L. (2000) Antiparallel leucine zipper-directed protein reassembly: Application to the green fluorescent protein. *J Am Chem Soc* **122:** 5658–9.
9. Rous B.A., Reaves B., Ihrke G., Briggs J.A., Gray S.R., Stephens D.J., Banting G., Luzio J.P. (2002) Role of adaptor complex AP-3 in targeting wild-type and mutated CD63 to lysosomes. *Mol Biol Cell* **13:** 1071–82.
10. Marchese A., Benovic J.L. (2001) Agonist-promoted ubiquitination of the G protein-coupled receptor CXCR4 mediates lysosomal sorting. *J Biol Chem* **276:** 45509–12.
11. Huskens D., Princen K., Schreiber M., Schols D. (2007) The role of N-glycosylation sites on the CXCR4 receptor for CXCL-12 binding and signaling and X4 HIV-1 viral infectivity. *Virology* **36:** 280–7.
12. Mori Y., Koike M., Moriishi E., Kawabata A., Tang H., Oyaizu H., Uchiyama Y., Yamanishi K. (2008) Human herpesvirus-6 induces MVB formation, and virus egress occurs by an exosomal release pathway. *Traffic* **9:** 1728–42.
13. Ageberg M., Lindmark A. (2003) Characterisation of the biosynthesis and processing of the neutrophil granule membrane protein CD63 in myeloid cells. *Clin Lab Haematol* **25:** 297–306.

T Cell–Mediated Control of Epstein-Barr Virus Infection in Humanized Mice

Misako Yajima,[1] Ken-Ichi Imadome,[1] Atsuko Nakagawa,[2] Satoru Watanabe,[3] Kazuo Terashima,[4] Hiroyuki Nakamura,[1] Mamoru Ito,[6] Norio Shimizu,[3] Naoki Yamamoto,[5] and Shigeyoshi Fujiwara[1]

[1]Department of Infectious Diseases, National Research Institute for Child Health and Development, and [2]Pathology Laboratory, Department of Clinical Laboratory Medicine, National Center for Child Health and Development, Setagaya-ku, [3]Department of Virology, Division of Medical Science, Medical Research Institute, and [4]Department of Pathology, Faculty of Medicine, Tokyo Medical and Dental University, Bunkyo-ku, and [5]AIDS Research Center, National Institute of Infectious Diseases, Shinjuku-ku, Tokyo, and [6]Central Institute for Experimental Animals, Kawasaki, Kanagawa, Japan

Humanized NOD/Shi-*scid*/interleukin-2Rγ^{null} (NOG) mice with full T cell development had significantly longer life span after Epstein-Barr virus (EBV) infection, compared with those with minimal T cell development. Removing CD3$^+$ or CD8$^+$ T cells from EBV-infected humanized mice by administration of anti-CD3 or anti-CD8 antibodies reduced their life span. CD8$^+$ T cells obtained from EBV-infected mice suppressed the outgrowth of autologous B cells isolated from uninfected mice and inoculated with EBV in vitro. These results indicate that humanized NOG mice are capable of T cell–mediated control of EBV infection and imply their usefulness as a tool to evaluate immunotherapeutic and prophylactic strategies for EBV infection.

Epstein-Barr virus (EBV) is a ubiquitous B-lymphotropic herpesvirus, and >90% of the adult population in the world is latently infected with the virus [1]. Although EBV is an important etiological factor in various malignancies, including endemic Burkitt lymphoma, Hodgkin lymphoma, and nasopharyngeal carcinoma, most EBV infection is asymptomatic and persists for life without any signs or symptoms. EBV has a unique ability to transform human B lymphocytes in vitro and to establish immortalized lymphoblastoid cell lines [2]. EBV-transformed lymphoblastoid cell lines express 9 viral proteins, most of which serve as efficient targets of EBV-specific T cell responses [2]. In immunologically competent hosts, therefore, EBV-transformed cells are readily removed by EBV-specific cytotoxic T lymphocytes [3], and EBV persistence is restricted to memory B cells, in which the expression of all viral proteins is shut down [4]. In immunocompromised hosts, however, EBV-infected B lymphoblasts can proliferate to cause lymphoproliferative disorder [1]. Thus, EBV persistence in human hosts is based on a fine balance between the host immunosurveillance, especially the function of EBV-specific cytotoxic T lymphocytes, and the replicative potential of EBV and the growth potential of EBV-infected cells.

Recently, we developed a new humanized mouse model of EBV infection, based on the NOD/Shi-*scid*/interleukin-2Rγ^{null} (NOG) mouse strain [5], that can reproduce key aspects of human EBV infection, such as lymphoproliferative disorder, asymptomatic persistent infection, and humoral and T cell–mediated immune responses [6]. In this model, inoculation with high-dose EBV (~1×10^3 50% transformation dose [TD_{50}]) resulted in the development of lymphoproliferative disorder, whereas inoculation with low-dose virus ($\leq 1 \times 10^1$ TD_{50}) tended to cause apparently asymptomatic persistent infection. Enzyme-linked immunospot assay and flow cytometry identified CD8$^+$ T cells that recognize autologous EBV-transformed lymphoblastoid cells and produce IFN-γ in a human major histocompatibility complex class I–restricted manner [6]. Although immune responses to EBV have been demonstrated in this NOG mouse model and other types of humanized mice [7, 8], whether these immune responses work functionally to control EBV infection has not been clarified. To address this issue, we examined whether T cells in humanized NOG mice have any influence on the survival of EBV-infected mice. We also tested whether CD8$^+$ T cells isolated from EBV-infected NOG mice have a capacity to suppress EBV-induced lymphocyte transformation.

Methods. NOG mice were obtained from the Central Institute for Experimental Animals, and cord blood samples were supplied by the Tokyo Cord Blood Bank after obtaining informed consent. Reconstitution of human immune system components was performed as described elsewhere [6, 9, 10]. In brief, CD34$^+$ human hematopoietic stem cells (HSCs) were isolated from cord blood with use of the MACS Direct CD34 Progenitor Cell Isolation Kit (Miltenyi Biotec), and 1×10^4–

Received 14 May 2009; accepted 19 June 2009; electronically published 15 October 2009.
Potential conflicts of interest: none reported.
Financial support: Ministry of Health, Labour and Welfare of Japan (H19-AIDS-003 and H21-AIDS-008) and a grant for the Research on Publicly Essential Drugs and Medical Devices from The Japan Health Sciences Foundation.
Reprints or correspondence: Dr. Shigeyoshi Fujiwara, Dept. of Infectious Diseases, National Research Institute for Child Health and Development, 2-10-1 Okura, Setagaya-ku, Tokyo 157-8535, Japan (shige@nch.go.jp).
The Journal of Infectious Diseases 2009;200:1611–15

0022-1899/2009/20010-0018$15.00
DOI: 10.1086/644644

1.2×10^5 cells/mouse of HSCs were transplanted in 6–10-week-old female NOG mice via the tail vein. The development of human blood cells in the peripheral blood was monitored by staining with monoclonal antibodies specific to human CD45RA, CD45RO, CD19, CD3, CD4, and CD8. NOG mice in which the human hematoimmune system was reconstituted are referred to here as humanized NOG mice. The term "lot" signifies a group of humanized mice derived from a single cord blood donor. Protocols of experiments with NOG mice were approved by the Institutional Animal Care and Use Committee of the National Institute of Infectious Diseases. The use of human materials in this research was approved by the In-

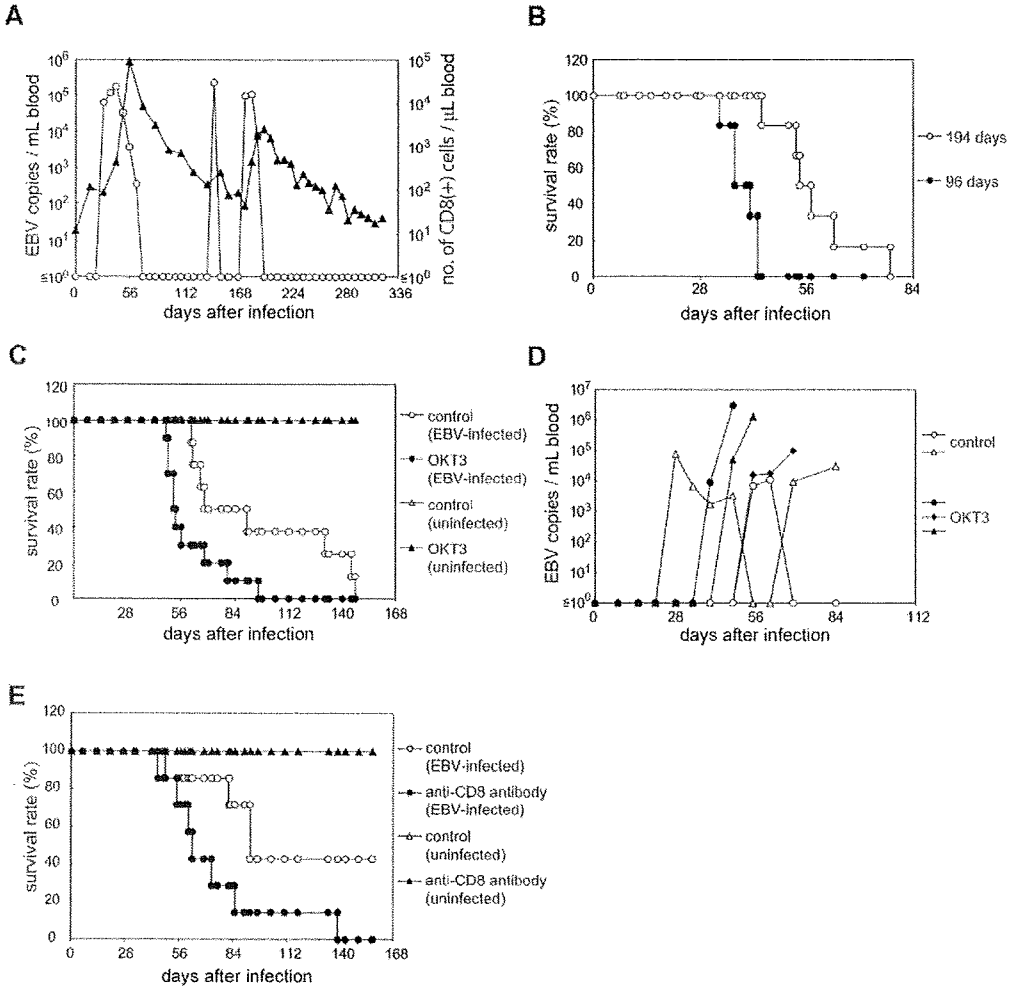

Figure 1. Evidence for T cell–mediated control of Epstein-Barr virus (EBV) infection in humanized NOD/Shi-*scid*/interleukin-2Rγ^{null} (NOG) mice. *A*, Associated changes in the number of CD8$^+$ T cells and viral DNA level in the peripheral blood of an EBV-infected humanized NOG mouse inoculated with EBV at ten 50% transformation dose (TD_{50}). The levels of EBV DNA *(open circles)* and CD8$^+$ T cells *(black triangles)* were monitored periodically. *B*, Survival curves of humanized NOG mice inoculated with EBV at different stages of reconstitution with human lymphocytes. Black circles represent mice inoculated with EBV (1×10^3 TD_{50}) at 96 days after transplantation with hematopoietic stem cells, and open circles represent mice inoculated at 194 days. *C*, Effect of depletion of T cells on the survival of EBV-infected humanized NOG mice. Black circles represent mice given daily intravenous injection with the OKT3 antibody (2 μg/mouse/day), starting at 21 days after infection, and open circles represent mice not given the antibody. Black triangles represent EBV-uninfected humanized NOG mice given OKT3 antibody, and open triangles represent such mice not given the antibody. *D*, Effect of depletion of T cells on the peripheral blood level of EBV DNA in humanized NOG mice. Black circles, black triangles, and black diamonds represent 3 humanized NOG mice inoculated with EBV (1×10^3 TD_{50}) that were treated with OKT3 as described in *C*, and open circles and open triangles represent such mice not treated with the antibody. Interruption of records indicates the death of a mouse. *E*, Effect of antibody specific to the CD8 molecule (B9.11) on the survival of EBV-infected humanized NOG mice. Black circles represent EBV-infected humanized NOG mice given daily intravenous injection with B9.11 (2 μg/mouse/day), starting at 21 days after infection, and open circles represent such mice not given the injection. Black triangles represent humanized NOG mice not infected with EBV that were given OKT3 antibody, and open triangles represent such mice not given the antibody.